Neuro-Oncology Advances
6(1), 1–12, 2024 | https://doi.org/10.1093/noajnl/vdad164 | Advance Access date 19 December 2023

TGF-β and BMP signaling are associated with the transformation of glioblastoma to gliosarcoma and then osteosarcoma

Aiguo Li[†], John C. Hancock[†,•], Martha Quezado, Susie Ahn, Nicole Briceno, Orieta Celiku[•], Surabhi Ranjan, Orwa Aboud, Nicole Colwell, Sun A. Kim, Edjah Nduom, Skyler Kuhn, Deric M. Park, Elizabeth Vera, Ken Aldape, Terri S. Armstrong, and Mark R. Gilbert[•]

Neuro-Oncology Branch, National Cancer Institute, National Institutes of Health (NIH), Bethesda, Maryland, USA (A.L., J.C.H., S.A., N.B., O.C., S.R., N.C., D.M.P., E.V., T.S.A., M.R.G.); Laboratory of Pathology, National Cancer Institute, NIH, Bethesda, Maryland, USA (M.Q., S.A.K., K.A.); Department of Neurology and Neurological Surgery, University of California, Davis, Sacramento, California, USA (O.A.); Surgical Neurology Branch, National Institute of Neurological Disorders and Stroke, NIH, Bethesda, Maryland, USA (E.N.); Research Technology Branch, National Institute of Allergy and Infectious Diseases, NIH, Bethesda, Maryland, USA (S.K.)

Corresponding Author: Mark A. Gilbert, MD, Neuro-Oncology Branch, National Cancer Institute, National Institutes of Health (NIH), Building 82, Room 235A, Bethesda, MD 20892 (mark.gilbert@nih.gov).

[†]These authors are co-first authors.

Abstract

Background. Gliosarcoma, an isocitrate dehydrogenase wildtype (IDH-WT) variant of glioblastoma, is defined by clonal biphasic differentiation into gliomatous and sarcomatous components. While the transformation from a glioblastoma to gliosarcoma is uncommon, the subsequent transformation to osteosarcoma is rare but may provide additional insights into the biology of these typically distinct cancers. We observed a patient initially diagnosed with glioblastoma, that differentiated into gliosarcoma at recurrence, and further evolved to osteosarcoma at the second relapse. Our objective was to characterize the molecular mechanisms of tumor progression associated with this phenotypic transformation.

Methods. Tumor samples were collected at all 3 stages of disease and RNA sequencing was performed to capture their transcriptomic profiles. Sequential clonal evolution was confirmed by the maintenance of an identical *PTEN* mutation throughout the tumor differentiation using the TSO500 gene panel. Publicly available datasets and the Nanostring nCounter technology were used to validate the results.

Results. The glioblastoma tumor from this patient possessed mixed features of all 3 TCGA-defined transcriptomic subtypes of an IDH-WT glioblastoma and a proportion of osteosarcoma signatures were upregulated in the original tumor. Analysis showed that enhanced transforming growth factor-β (TGF-β) and bone morphogenic protein signaling was associated with tumor transformation. Regulatory network analysis revealed that TGF-β family signaling committed the lineage tumor to osteogenesis by stimulating the expression of runt-related transcription factor 2 (RUNX2), a master regulator of bone formation.

Conclusions. This unusual clinical case provided an opportunity to explore the modulators of longitudinal sarcomatous transformation, potentially uncovering markers indicating predisposition to this change and identification of novel therapeutic targets.

Key Points

- Transforming growth factor-β (TGF-β) and bone morphogenic protein (BMP) signaling are associated with the glioblastoma to gliosarcoma transition in a clinical case that progressed to osteosarcoma.
- Primary bone osteosarcoma genes were expressed in the original glioblastoma.

Importance of the Study

Knowledge of the mechanism of the gliosarcoma transformation from glioblastoma is limited. This study provides the first comprehensive exploration of the underlying pathways leading to this transformation, within the context of a glioblastoma transforming to gliosarcoma and then ultimately to an unequivocal osteosarcoma. After RNA sequencing and network analysis, transforming growth factor-β (TGF-β) and bone morphogenic protein (BMP) signaling were found associated with this transition, modulating RUNX2 expression and likely leading to osteosarcoma. We also elucidated the relationship between TGF-β and its downstream regulators and signaling pathways. Primary bone osteosarcoma genes were expressed in the original glioblastoma and a majority were expressed in the subsequent gliosarcoma and osteosarcoma, implying that osteogenic origination commenced within the early stages of the disease progression. This mechanism has not been discussed previously in the treatment of gliosarcoma, as the ultimate change to osteosarcoma enabled the gliosarcoma transformation to be interrogated as an intermediate step (rather than a typical end-stage of disease progression).

Glioblastoma is a primary brain malignancy characterized by high heterogeneity, invasiveness, and resistance to current therapies, with a median survival of approximately 15 months.[1–3] Molecular subtyping aids our understanding toward tumor biology and improves prediction of clinical outcomes,[4] but the evolving classification models do not fully recapitulate tumor heterogeneity and longitudinal malignant transformation. The existence of multipotent glioma stem cells in the tumor leads to multiple lineage commitments, further compounding uncertainties about longitudinal progression.[5]

Gliosarcoma, a WHO-established variant of IDH-WT glioblastoma, accounts for approximately 2% of all diffuse glioma.[6–8] The WHO 2021 guidelines have defined gliosarcoma as a subtype of glioblastoma.[9] Primary gliosarcomas frequently arise de novo with a predilection for the temporal lobes and secondary gliosarcoma develops after cranial irradiation for glioblastoma.[3,8] The invasion of dura and extracranial metastases are more common in gliosarcoma than glioblastoma with potential prognostic implications,[8,10–12] although some studies showed no significant differences in overall survival between gliosarcoma and glioblastoma.[2,13] In many cases the 2 tumor types share identical clinical and radiological features and are clinically managed under similar or identical protocols, with surgery, radiation, and chemotherapy.[13–15] Gliosarcoma histologically shows a biphasic pattern composition displaying adjacent regions of gliomatous and sarcomatous differentiation with mesenchymal components.[4,10,16] The glial component expresses glial fibrillary acidic protein (GFAP) and is reticulin-poor, while sarcomatous lacks GFAP and is reticulin-rich.[3] Clinically, these distinct features have been used to differentiate between the glioblastoma and gliosarcoma cases.[3,17,18] Other types of rare transformations of gliosarcoma include chondrosarcoma, angiosarcoma, osteosarcoma, and liposarcomatous, myosarcomatous, leiomyomatous, and neuroectodermal tumors.[14,15,18–20]

Genetically, gliosarcoma is unstable, with more frequent TP53 mutations,[7,10,16] and a high rate of loss of heterozygosity at 10q (88%).[16] Poorer survival among TP53-mutated gliosarcoma patients has been reported, thus it has been diagnostically divided into TP53 mutated and intact (wildtype) gliosarcoma subtypes.[10] The reported incidence of TERT promoter mutations in gliosarcoma is 83%,[16] PTEN mutation (28.6–45%) and $P16^{INK4alpha}$ homozygous deletions is 37%.[14,15] EGFR amplification was only found in 4% of gliosarcomas, versus 40% in primary glioblastomas[14,21] and isocitrate dehydrogenase (IDH) mutations are rare in gliosarcoma.[15] It has been suggested that biomarkers of gliosarcoma with potential therapeutic implications include PTEN, EGFR, BRAF, CDKN2A, and NF1.[22] MGMT promoter methylation is more frequent in glioblastoma than in primary gliosarcoma[6,11] and a trend of increased survival in patients with hypermethylated MGMT promoter by improving the efficacy of TMZ treatment was reported.[6,23]

Knowledge of the underlying molecular etiology pertaining to gliosarcoma transformation from glioblastoma is limited. The evolution to gliosarcoma has been associated with altered pathways in MAPK signaling (EGFR, RASGRF2, and TP53), phosphatidylinositol/calcium signaling (CACAN1s, PLCs, and ITPRs), and focal adhesion/tight junction (PTEN and PAK3) pathways.[10,24] Mesenchymal transformation in gliosarcoma is associated with SNAI2, TWIST1, and MMP-2/9 upregulation.[25] Current consensus on the cellular origin of gliosarcoma supports the monoclonal theory,

that both glial and mesenchymal elements may be derived from a common neoplastic neuroectodermal precursor.[26]

The differentiation of gliosarcoma into osteosarcoma is rare and has been reported in very few cases.[17,20,27–31] Morphologically, the occurrence of osseous elements is described as a process of tumor necrosis, calcification, calcification of necrotic foci, and secondary ossification of the calcified tissue.[17,27] The cellular origin of the osseous element has been described as a metaplastic change of the mesenchymal stroma and it has been reported that radiation contributes to the osseous differentiation.[14,30]

Here we describe a patient initially diagnosed with glioblastoma, which transformed into gliosarcoma at recurrence and further evolved into an osteosarcoma at second disease relapse. This unusual case highlights the comprehensive evolution of this disease and facilitates our growing understanding of the molecular genetics of glioblastoma and its rare variants. Our objectives were to characterize the radiologic and histopathologic features of this rare tumor, delineate the molecular mechanisms of tumor progression associated with morphological and phenotypic transformations, and identify possible pathways of disease transformation.

Materials and Methods

Tumor Specimen Acquisition

The initial surgical resection was performed outside the National Institutes of Health (NIH) Clinical Center, and the second and third tumor resections were carried out at the NIH Clinical Center. The patient was enrolled after signing informed consent to participate in the Institutional Review Board approved Neuro-Oncology Branch Natural History Study (NCT02851706, PI: TS Armstrong) which permits to collection, analysis, and publication of the patient's medical history and biologic specimens including tumor samples.

Neuroimaging

MRI with and without gadolinium contrast was performed on a 1.5 T MR scanner (Sigma, General Electric) or a similar scanner, and a 3T (Philips Medical Systems) or similar scanner as part of clinical care. Sequences performed included pre and postcontrast fluid inversion recovery (FLAIR), T2*-weighted imaging using both conventional GRE and susceptibility-weighted imaging, isotropic diffusion-weighted imaging (DWI), and apparent diffusion coefficient maps. All MRI scans were interpreted by a clinical radiologist.

Histopathological Staining and Molecular Diagnosis

Hematoxylin and eosin (H&E), GFAP antibody, and reticulin special stain with prediluted solution were used to stain the sections per manufacturer guidelines (https://lifescience.roche.com). Microscopic sections from each surgery were reviewed by a neuropathologist (MMQ) to determine the cellular morphology of the tumor. Gene panel profiling was done using the Illumina TrueSight Oncology 500 (TSO500) platform (https://www.illumina.com) by the National Cancer Institute's (NCI) Molecular Diagnosis Laboratory in the Laboratory of Pathology. We carried out the TSO500 panel analysis for all 3 tumor stages, but only the glioblastoma tumor of this case yielded outputs that passed the data quality control. The TSO500 panel analysis does not include MGMT methylation.

RNA Extraction and Sequencing

Total RNA was extracted from the FFPE slides using the RNeasy FFPE kit (Qiagen). RNA integrity was measured on an Agilent 2100 BioAnalyzer using the RNA 6000 Pico kit (Agilent Technologies). In addition, the DV200 was assessed and used to determine the quality of total RNA samples for sequencing with a cutoff greater than 30%. The transcriptome library was prepared using the Illumina TrueSeq RNA Access kit following the manufacturer's instructions. The library was sequenced on Illumina HiSeq 2500 using 125 bp paired-end reads targeting a sequence coverage of 50–60 million per sample carried out by NCI's Advanced Technology Research Facilities.

RNA-Seq Data Analysis

Strand-specific RNA-seq reads were analyzed using CCBR Pipeliner (https://github.com/CCBR/Pipeliner). The pipeline steps include several tasks: sequencing reads quality control and grooming, alignment to the reference genome, feature quantification, and differentially expressed gene identification. Initially, sequencing reads that passed quality control thresholds were trimmed of adaptor sequences using a trimmomatic algorithm; STAR was then used for genomic alignment to the human reference genome version HG19; the transcripts were quantified using RSEM algorithms; and differentially expressed genes were determined using EdgeR, DESeq2, and limma/voom methods. We derived differentially expressed genes using thresholds of FDR ≤ 0.05 and absolute fold changes ≥ 1.5 across all 3 methods by contrasting osteosarcoma to gliosarcoma, gliosarcoma to glioblastoma, and osteosarcoma to glioblastoma, as well as each tumor stage to the rest of the samples. Genes correlated with tumor progression were identified using a Pearson correlation with a threshold of FDR < 0.05 and a correlation coefficient (r) > 0.45.

Functional Pathway and Network Analysis

Pathway and network analysis was carried out using Ingenuity Pathway Analysis (IPA; www.qiagenbioinformatics.com), and Cytoscape (http://www.cytoscape.org). The differentially expressed genes (either up- or downregulated) were uploaded into IPA and core analysis was performed for each contrast. Enriched canonical pathways, upstream interaction partners and regulators, and associated diseases and functions were

inspected to elucidate underlying molecular functions. In addition, pathway overlay and network analysis were performed to further investigate biological functions. Cytoscape analysis was performed on glioblastoma and osteosarcoma networks constructed using the corresponding gene sets.

Single Sample Gene Set and Gene Set Enrichment Analysis (ssGSEA and GSEA)

To understand the underlying molecular mechanisms during tumor differentiation, we carried out ssGSEA and GSEA by contrasting osteosarcoma to gliosarcoma, gliosarcoma to glioblastoma, and osteosarcoma to glioblastoma (http://software.broadinstitute.org/gsea/index.jsp). ssGSEA was performed using the R package GSVA[32] and the Gene Ontology database. Contrasts between tumor stages were determined using outputs from GSVA, and q-values < 0.05 were used to identify enriched features and functions. GSEA analysis was done using the JavaGSEA desktop application (GSEA ver. 3.0).[33] For GSEA, C2 curated gene sets of less than 10 genes or greater than 300 genes were excluded. Given that the number of samples in this study was small, the P-values were calculated by permutating the genes 1000 times to identify enriched gene sets. q-Values less than 0.05 from GSEA outputs were used as the threshold to determine up- or downregulated genesets for each comparison. R (ver. 3.5.2) was used to cluster and summarize the GSEA outputs.

Data Analysis and Validation From Public Resources

RNA-seq data analysis was performed using CCBR Pipeliner and analysis using IPA, Cytoscape and GSEA (details in Supplementary Materials). For validation analyses, we first downloaded an RNA-Seq dataset of IDH wildtype glioblastoma tumors from Genomic Data Commons (https://datacommons.cancer.gov/) with assigned molecular subtypes,[4,34] then normalized with our data and carried out batch correction. Second, we downloaded a primary bone osteosarcoma dataset (GSE99671) from gene expression omnibus (GEO).[35,36] A paired t-test was used to derive an osteosarcoma signature gene set, and a global unsupervised PCA analysis was used to characterize the patient's tumor. We also downloaded a gliosarcoma gene expression data set (GSE8692)[37] to verify our findings that transforming growth factor-β (TGF-β) is the driving force for glioblastoma transition to gliosarcoma. Lastly, we used an internal dataset from our previous publication to derive glioblastoma overexpressed genes compared with normal brain tissue.[38]

Nanostring nCounter Validation

Custom probe sets for 100 selected genes were designed and manufactured by NanoString Technologies. FFPE RNA was hybridized with reporter and capture probes at 65°C for 16 h (NanoString Technologies). The amount of input FFPE RNA was adjusted based on the DV200, as recommended by the manufacturer. Posthybridization processing and data collection on the NanoString nCounter Analysis System was conducted at the CCR Genomics Core at the NCI.

Results

Case Description and Clinical Characteristics

The patient was a 56-year-old woman who initially presented with episodes of confusion and expressive aphasia for 1 month. Brain imaging revealed a large left parietal contrast-enhanced mass (Figure 1A-I). Histopathology showed a high-grade neoplasm (Figure 1B-I) with variable morphology and a prominent small cell phenotype that was strongly GFAP-positive (Figure 1C-I) and reticulin-negative glia (data not shown) consistent with glioblastoma (Figure 1B-I). Areas of atypical mesenchymal proliferation were noted that were reticulin-rich and GFAP-positive. Treatment after surgery included 6 weeks of concurrent chemoradiotherapy with temozolomide, followed by 12 cycles of adjuvant temozolomide. Worsening expressive aphasia and cognitive impairment and imaging revealed concern for tumor recurrence led to a reresection of the mass. Histopathology now confirmed transformation to gliosarcoma (Figure 1A-II) as evidenced by mesenchymal sarcomatous changes (Figure 1B-II and C-II), that was reticulin-rich (Figure 4B-II) and GFAP-negative glia (data not shown). The patient was treated with oral sunitinib with a transient imaging response. A second recurrence, 17 months from the initial diagnosis was found as the patient developed right-sided numbness along with incoordination. Imaging showed further tumor growth and significant mass adhesion to the overlying dura (Figure 1A-III). A surgical resection was performed demonstrating the mass to be entirely calcified and the histopathology revealed a malignant osteoid-producing mesenchymal neoplasm (Figure 1B-III). Immunopathological diagnosis confirmed transformation to osteosarcoma (Figure 1A-III and B-III).

The Glioblastoma Tumor Resembled the Proneural Subtype but Possessed Strong Classical and Mesenchymal Characteristics

Molecular studies of this case identified a deleterious PTEN mutation (p.R130G) at the exon 4 region, and the RNA-Seq data revealed that the PTEN mutation persisted through all 3 differentiation stages (Supplementary Figure 1A). To elucidate the tumor-intrinsic transcriptional heterogeneities of this patient over longitudinal transformation, we carried out RNA-Seq of 9 tumor samples from 3 differentiation stages. The unsupervised principal component analysis (PCA) of RNA-Seq data projected global transcriptomic separation between the stages (Figure 1D-I). The heatmap of over 7000 differentially expressed genes indicated that initially upregulated genes in the glioblastoma tumor became inactive during differentiation, while most of the other genes were commonly upregulated in the gliosarcoma and osteosarcoma tumors, indicating an inherent molecular similarity of the 2 recurrent tumors (Figure 1D-III).

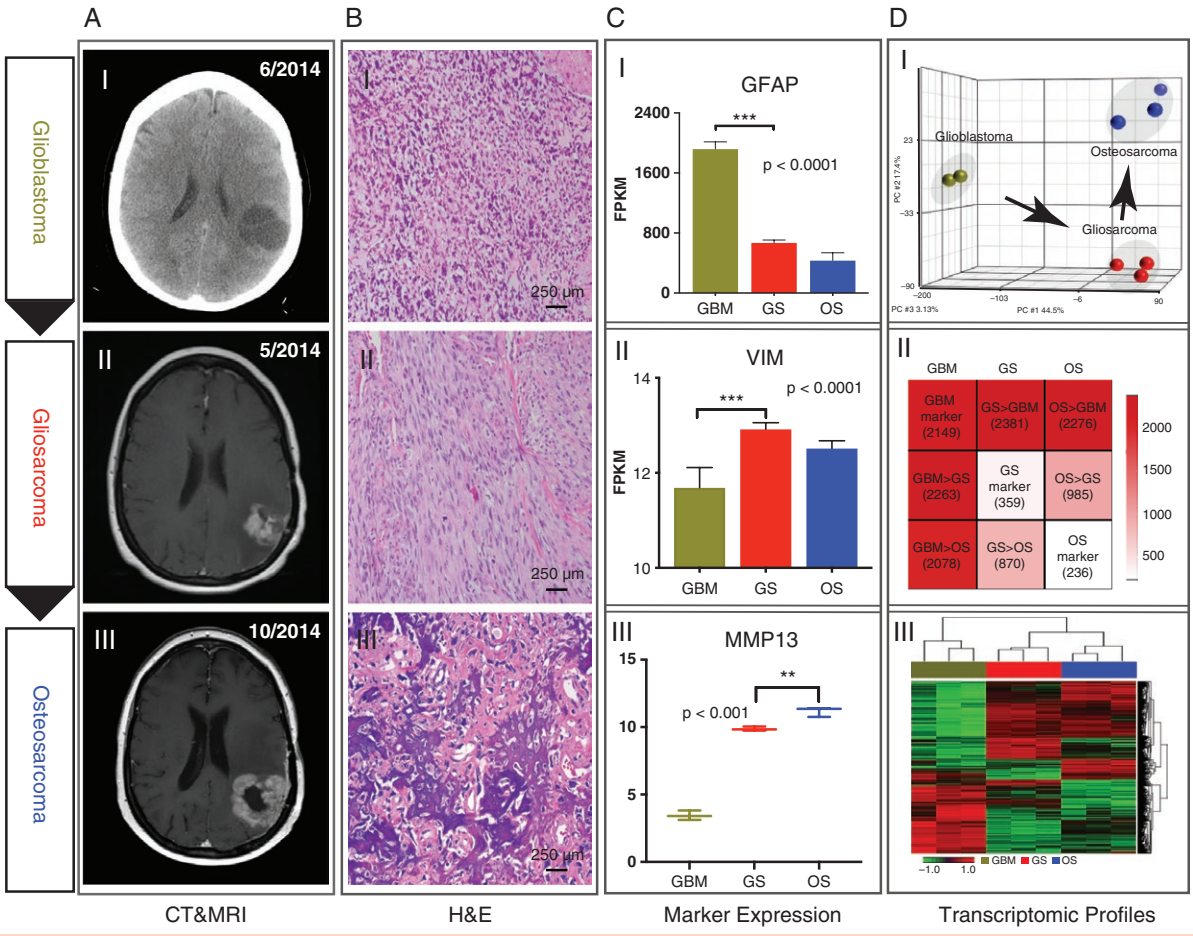

Figure 1. Radiographic and immunohistochemical characteristics of the tumor and its global transcriptomic profiles. (A) Axial images of the tumor on initial presentation, on second and third relapse, respectively. Preoperative CT head without contrast with left parietal hypodensity of pathology glioblastoma (A-I). MRI brain axial T1 postcontrast with recurrent contrast-enhancing lesion with surrounding hypointensity vasogenic edema (A-II). MRI brain axial T1 postcontrast with same-site recurrent contrast-enhancing lesion with worsening surrounding edema (A-III). (B) Microscopic images of the tumor from glioblastoma with microvascular proliferation and GFAP-positive (10×) (B-I), from gliosarcoma with reticulin stain positive and spindle cell morphology (10×) (B-II), and from osteosarcoma with malignant osteoid formation (10×) (B-III). (C) Representative marker gene expression in FPKM at 3 tumor stages. (D) Transcriptomic profiles during tumor progression. Unsupervised principal component analysis of the tumor transcriptomic profiles across 3 differentiation stages reveal 3 sparsely separated clusters (D-I). Differential expression matrix based on genes identified during tumor transformation. The values are numbers of genes whose expression is enriched in the A group of the contrasts with B (A > B) using thresholds of false discovery rate < 0.05 across DEseq2, EdgeR and Limma/voom methods and absolute fold changes ≥ 1.5. The gene numbers in diagonal were derived by the group contrasted to the rest of the samples (D-II). Hierarchical clustering analysis of all differentially expressed genes across 3 comparisons during tumor progression. Euclidean distance and complete linkage methods were used in the analysis (D-III).

To compare the glioblastoma stage of this case to known glioblastoma molecular subtypes, we performed supervised clustering using the 150 classifiers of IDH-wildtype glioblastoma,[34] which resulted in all 3 glioblastoma samples to be projected on the boundary areas of classical, proneural, and mesenchymal subtypes (Figure 2B). Other classification approaches similarly yielded a mixed subtype (Supplementary Table 1). When considering all stages, supervised clustering indicated that the glioblastoma tumor most resembled the proneural subtype with a highly enriched expression of proneural signature genes, but then shifted to the mesenchymal subtype after transforming into a gliosarcoma (Figure 2A). This finding was further affirmed using the original Verhaak's 800 classifier approach into 4 glioblastoma subtypes (Supplementary Figure 2A).[4] The tumor held attributes of the proneural subtype by having highly expressed oligodendrocyte development genes (OLIG2 and NKX2-2) (Figure 2C) and the proneural development gene SOX2 (Supplementary Figure 1E). As in the proneural subtype, highly expressed OLIG2 in the tumor negatively correlated with the tumor suppressor CDKN1A ($r = -0.94$, $P < -.000015$), leading to increased proliferation, as shown in the histopathological stain (Figure 1B-I). While the proneural signature was the most pronounced, this tumor imitated the classical subtype with enhanced NOTCH signaling (NOTCH1/3, DLL1,3,4) neural activities (Figures 2D and 3A, Supplementary Figures 1B and 4A), highly expressed

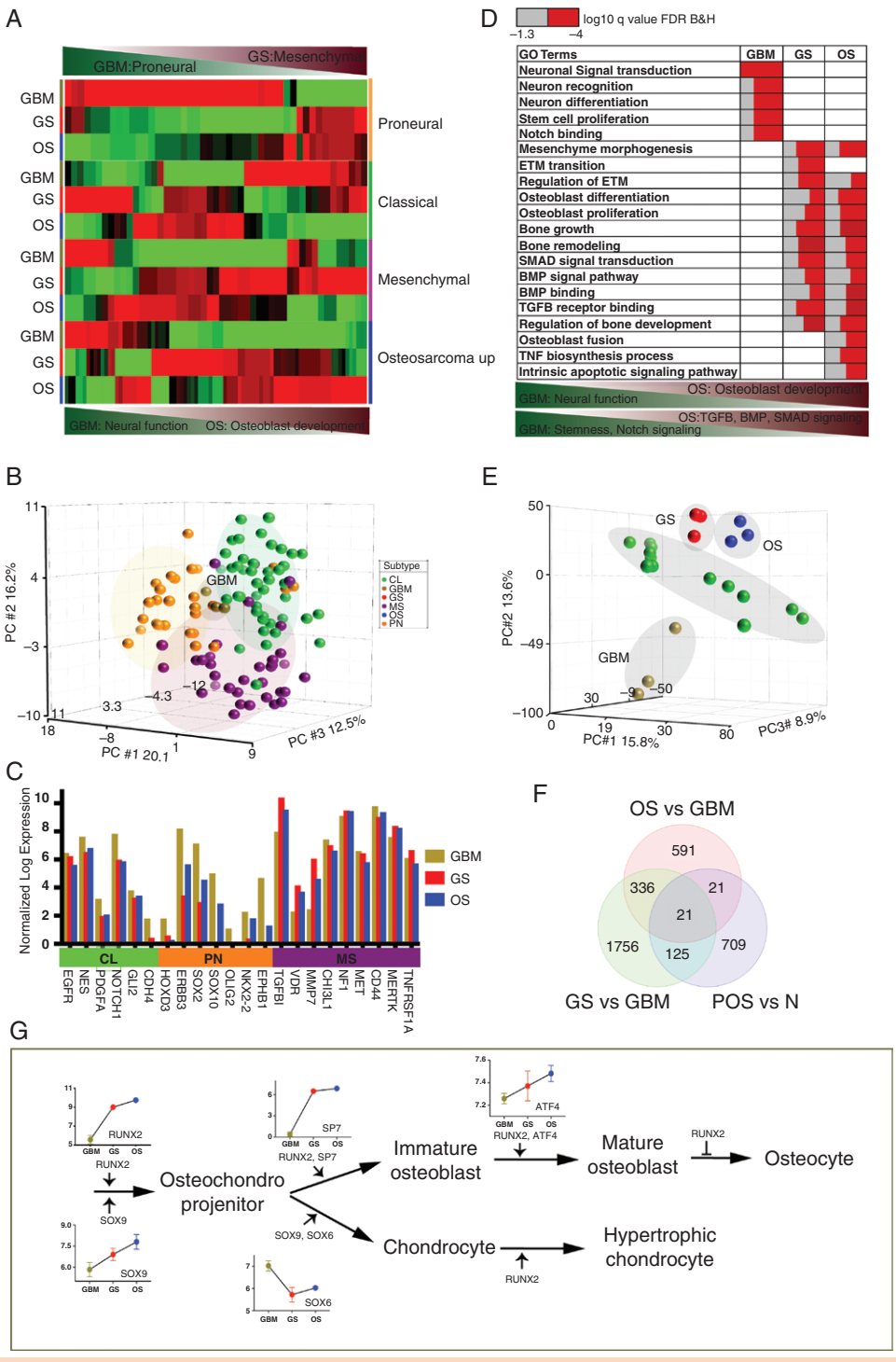

Figure 2. Characterization of tumors using transcriptomic classification systems. (A) Supervised hierarchical clustering analyses of 3 tumor stages using Wang's 3-subtype classifiers and supervised hierarchical clustering analyses of 3 tumor stages using osteosarcoma signature genes. (B) The principal component analysis projected the 3 glioblastoma tumor samples to the boundary area of the TCGA glioblastoma patients previously assigned to Wang's 3 molecular subtypes. (C) Expression of the subtype classifiers in our glioblastoma case. (D) Upregulated gene ontology (GO) terms during tumor progression identified by ssGSEA using the GO database. The glioblastoma tumor is enriched with neural functions and stem cell activities and enhanced NOTCH signaling. Gliosarcoma and osteosarcoma tumors are featured with osteoblast development and bone growth, and BMP, TGFB, and SMAD signaling. (E) Unsupervised principal component analysis of bone-originated osteosarcoma tumors and our primary and recurrent tumors. (F) Venn diagram of osteosarcoma-related genes in primary osteosarcoma tumors and in our recurrent tumors. (G) Bone differentiation modulated by the RUNX2 transcription factor.

EGFR, PDGFA, GLI2, and CDH4 genes (Figure 2C) and vigorous stemness ingredients (NES, PROM1, and MSI1/2) (Supplementary Figures 1B and 4A). However, as our subtype prediction revealed (Supplementary Table 1), the most prominent features of this glioblastoma were its enhanced expression of mesenchymal markers (MET and CHI3L1), mesenchymal signature genes (CD44, MERTK, MMP7/9/13, VDR, VEGFA, and TGFBI), the NFKB pathway (TRADD and TNFRSF1A) (Figure 1C-III, 2C, Supplementary Figure 1D), GPCR signaling, cell adhesion genes, and ABC transporter activity (Supplementary Figure 1C). Hence, this tumor possessed mixed features of classical, proneural, and mesenchymal subtypes.

Runt-Related Transcription Factor (RUNX2) Regulated Osteosarcoma Tumor Differentiation

To gauge whether the osteosarcoma that ultimately developed in this patient was similar to primary bone osteosarcoma, we downloaded a dataset from GEO (GSE99671)[35] containing RNA-Seq data from 18 tumor-normal pairs (FFT) and 18 formalin-fixed paraffin-embedded bone osteosarcomas (FFPE). PCA analysis revealed 4 sparsely separated clusters, indicating that the present osteosarcoma differed from primary bone osteosarcoma (Figure 2E). To confirm this finding, we further derived a bone osteosarcoma signature of roughly 800 genes from the FFT dataset. Again, the signature showed poor overlap with the upregulated genes in both the osteosarcoma and gliosarcoma tumors of this case (Figure 2F). We further mapped this signature to our dataset and the heatmap showed that a small portion of signature genes was expressed early at the glioblastoma stage, and more than half of the signature genes were expressed in both the gliosarcoma and osteosarcoma tumors (Figure 2A). Comparing glioblastoma overexpressed genes with primary osteosarcoma overexpressed genes also shows some degree of overlapped genes, indicating an early commencement of the osteogenic progress in this patient (Supplementary Figure 4B).

RUNX2 defines the transcriptional regulatory network of normal bone development and induces differentiation of multipotent mesenchymal cells into osteoblasts in tumor transformation.[39,40] Our regulatory network analysis identified RUNX2 as a top transcription factor of osteoblast differentiation (Supplementary Figure 3A) and gene-interaction network analysis pinpointed RUNX2 as a highly connected hub gene in the gliosarcoma tumor network (Supplementary Figure 2H). Pearson correlation analysis significantly associated RUNX2 expression with tumor progression ($r = 0.93$, $P < .0002$). We examined RUNX2 function in regulating the bone formation of our tumor and checked its conformity with normal osteoblastogenesis. The analysis unfolded that RUNX2 activated downstream transcription factors SP7, ATF4, and SOX6, leading to osteoblast and chondrocyte formation. The tumor shared an identical regulatory network with normal bone formation (Figure 2G). Accompanying the tumor transformation, many bone formation-related genes (BMP2/4, SPARC, SOX9, PTH1R, FRZB, PLOD2, and COL11A1), as well as mesenchymal markers (MMP13 and SERPINE1/2), were highly expressed in the recurrent tumors (Figures 1C-III and 3E, Supplementary Figure 3B and E). In addition, the osteosarcoma tumor exhibited necrosis with upregulated HIF signaling pathways (Figure 3F, Supplementary Figure 3C and D). HIF1A and EGLN3 (a cellular oxygen sensor) were both upregulated in this tumor (Supplementary Figure 3B). We also identified upregulated WNT signaling and hedgehog signaling via ssGSEA analysis (Figure 3G, Supplementary Figures 2B and 3D).

TGF-β and BMP Signaling Modulated the Tumor Transformation From Glioblastoma to Gliosarcoma and Then to Osteosarcoma

Our comprehensive analysis revealed that TGF-β was a key regulator of the glioblastoma to gliosarcoma transformation ($P = 3.59E-43$) (Figure 3C). We found that all TGF-β ligands (TGFB1, TGFB2, TGFB3, and TGFBI) and TGF-β receptors (TGFBR1 and TGFBR2, but not TGFBR3) were upregulated in the gliosarcoma tumor. TGFBR3, a sequencer of TGF-β signaling, was downregulated at this stage (Supplementary Figure 2E). Furthermore, TGF-β downstream regulators, such as SMAD3/7, CTNNB1, FOS, and CEBPB (derived from the IPA knowledge base) were all significantly upregulated in the gliosarcoma tumor (Figure 3C). GSEA also affirmed this finding by identifying 7 TGF-β signaling pathways or gene sets significantly upregulated in the gliosarcoma (Figure 3D, Supplementary Figure 2C). In addition, we pooled together a TGF-β target gene set with more than 600 genes[41–43] and their expression was also upregulated during tumor differentiation to the gliosarcoma (Supplementary Figure 2D, upper).

To validate these findings, a microarray data set containing 4 glioblastomas, 2 gliosarcomas, and 1 secondary gliosarcoma (transformed from glioblastoma) was downloaded (GSE8692).[37] The TGF-β ligands, their cognate receptors, as well as their target genes, were also upregulated (Supplementary Figure 2D, lower and 2F). Regulatory network analysis identified the upregulation of BMP4, a secreted ligand of the TGF-β superfamily which plays a critical role in bone and cartilage development and can activate the expression of SMAD3, CTNNB1, and RUNX2 (Figure 3G and C, Supplementary Figure 2B). Furthermore, NanoString's nCounter technology was used to confirm the RNA-Seq results from this patient and compare the results to other independent tumors (8 glioblastomas and 7 gliosarcomas). The results validated our previous findings (Figure 3H, Supplementary Figure 4A).

Discussion

We propose that TGF-β and bone morphogenic protein (BMP) signaling play a role in driving the glioblastoma to gliosarcoma transition, modulating RUNX2 expression, and framing osteosarcoma differentiation (Figure 4A and B). RUNX2, as a master bone formation transcription factor, potentially drove the second recurrence from gliosarcoma to osteosarcoma in this patient. The paramount downstream transcription factors provoked by TGF-β and BMP signaling (direct or indirect) are CTNNB1, SMAD3/6, SOX9,

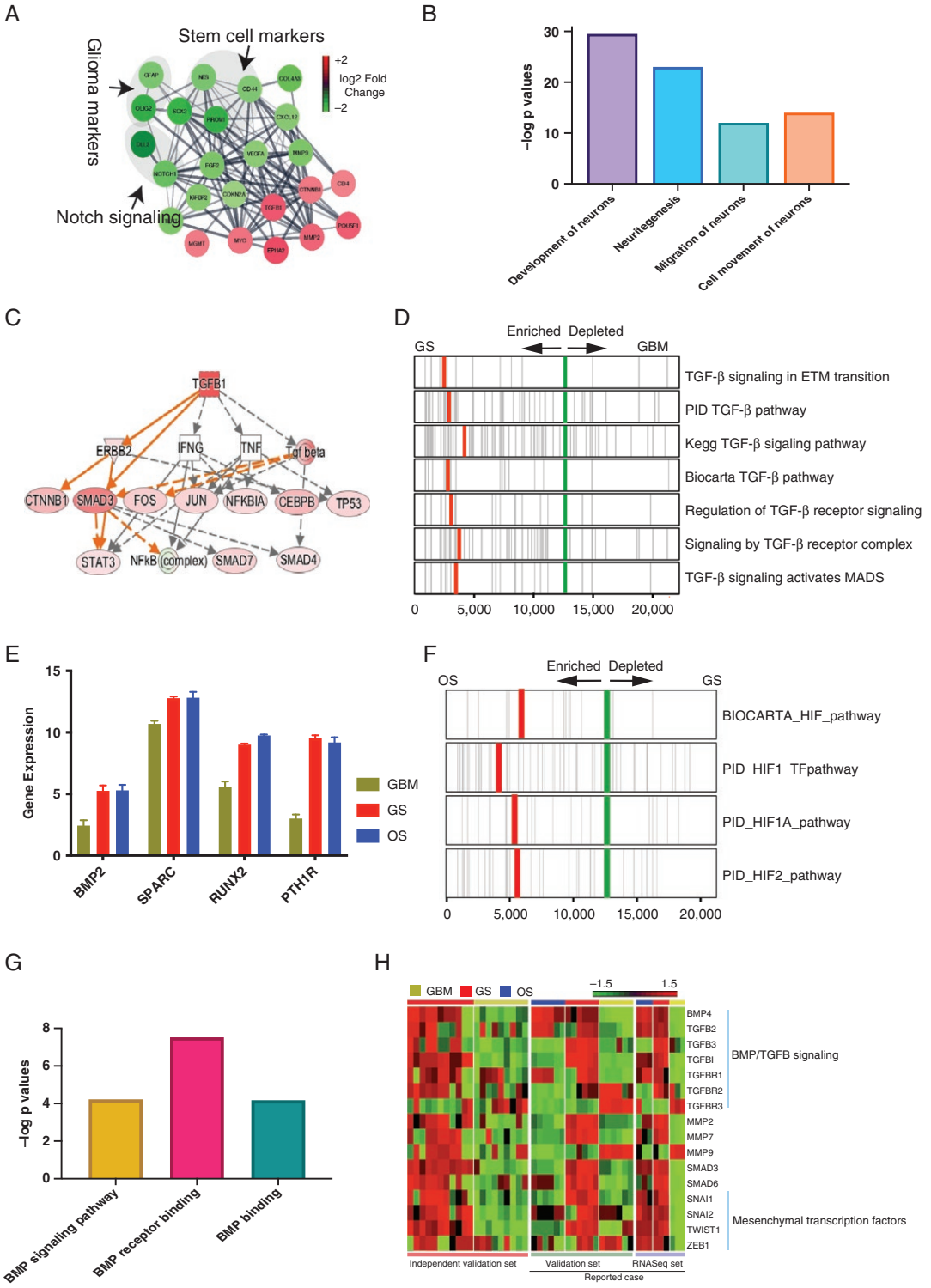

Figure 3. Molecular characteristics of tumors across 3 differentiation stages. (A) Glioblastoma network of the tumor as compared to gliosarcoma. Red refers to upregulated genes in gliosarcoma, green refers to upregulated genes in glioblastoma. (B) Upregulated genesets related to neuron activities in glioblastoma tumor derived by IPA analysis. (C) TGF-β regulatory network derived from IPA network analysis. Red refers to upregulated in gliosarcoma tumor. (D) TGF-β-related signaling pathways and genesets significantly upregulated in gliosarcoma tumor (FDR < 0.05). The green vertical line indicates where the expression correlation changes direction. The red vertical line indicates where the leading-edge set starts. (E) Genes involved in bone formation. (F) HIF signaling pathways upregulated in osteosarcoma tumor identified by GSEA analysis. The green vertical line indicates where the expression correlation changes direction. The red vertical line indicates where the leading-edge set starts. The bars on the left are the normalized enrichment scores. (G) Enhanced BMP signaling activities in gliosarcoma tumor identified by ssGSEA. (H) Gene expression validation of genes in BMP/TGFB signaling and mesenchymal transcription factors in an independent set and in the reported case.

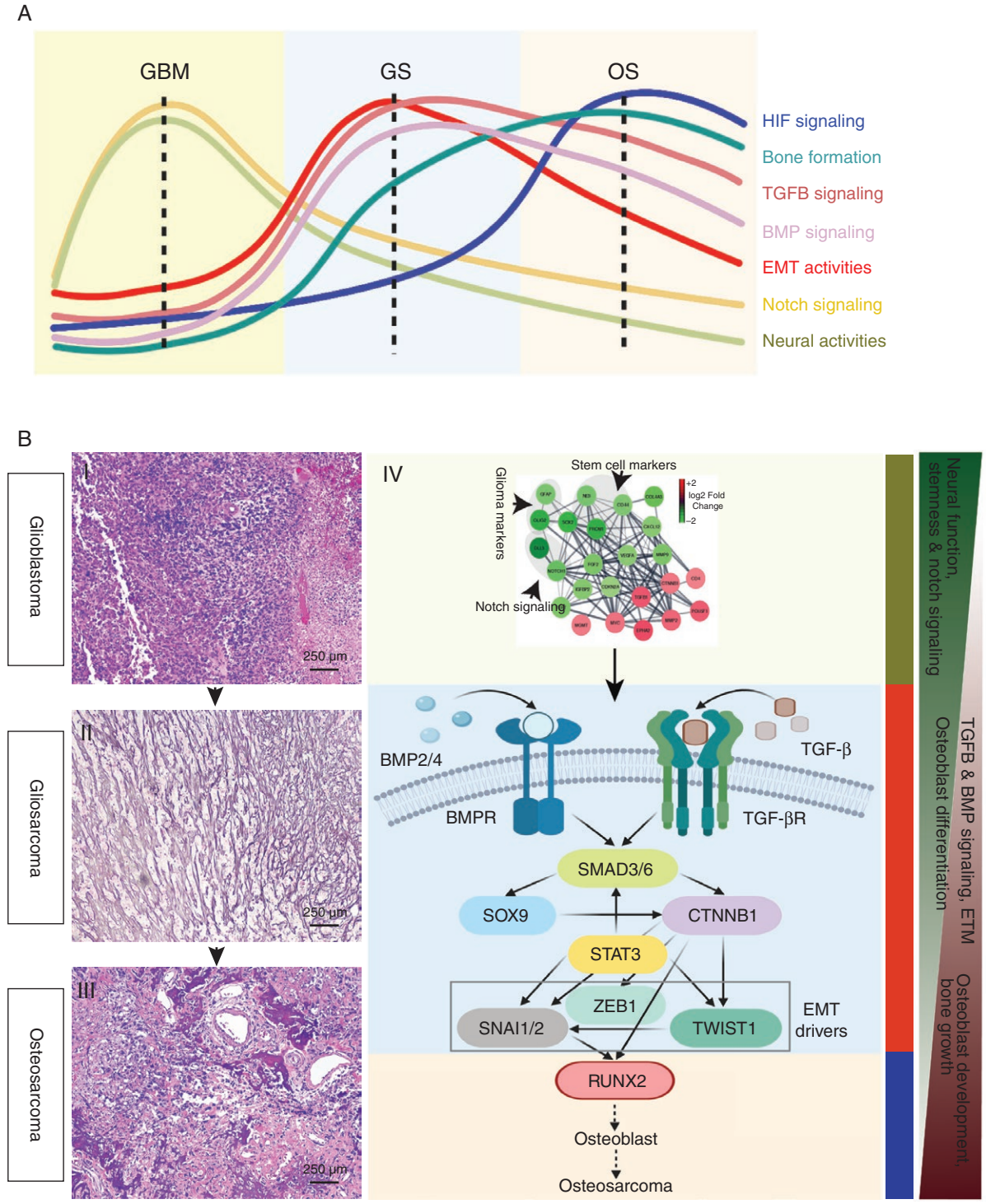

Figure 4. Molecular mechanisms driving tumor progression and the proposed regulatory network. (A) Molecular features and activities associated with tumor stages. (B) Proposed regulatory network driving the tumor differentiation and transformation.

STAT3, ZEB1, SNAI1/2, TWIST1, and RUNX2. CTNNB1, as an essential element of the WNT signaling pathway, regulates the expression of mesenchymal transcription factors SNAI1/2 and TWIST1 and contributes to the formation of the malignant mesenchymal features in the recurrent gliosarcoma (Figure 4A and B). The expression of these mesenchymal regulators further modulated RUNX2 expression, resulting in bone differentiation and formation. Primary bone osteosarcoma genes were expressed in the original glioblastoma and a majority were expressed in the

subsequent gliosarcoma and osteosarcoma, implying that osteogenic origination commenced within the early stages of the disease progression.

The characteristics of coexisting mesenchymal stem cells and multipotent cancer stem cells may have potentiated the differentiation of this tumor. The original glioblastoma had enhanced NOTCH signaling and the stem cell genes NES, SOX2, PROM1, and MSI1/2. TGF-β superfamily signaling orchestrates a wide array of cellular processes both in tumor and normal development. TGF-β signaling is involved in defining the mesenchymal stem cell differentiation path[44,45] and in the regulation of epithelial–mesenchymal transition in lung cancer and in mesothelioma.[46,47] TGF-β/BMP signaling play a role in osteoblastogenesis and bone formation.[48,49] TGF-β signaling triggers downstream SMADS, CTNNB1, and MYC and FOS signaling, which could have led to the malignant induction of a proneural–mesenchymal transition in this tumor by enhancing the expression of 4 mesenchymal transcriptional factors (TWIST1, SNAI1, SNAI2, and ZEB1) (Supplementary Figure 2G).[25,50] These transcription factors induced reprogramming and activated the transcription of the mesenchymal signature in the recurrent gliosarcoma tumor.[10,25,46] On the other hand, the multipotent mesenchymal stem cells have the capacity to differentiate into several cell lineages.[45] The commitment to a given lineage and differentiation progression along these lineages is controlled by specific transcription factors and tightly regulated by interactions with other cells in response to cellular and extracellular signals.[46,49] In our case, osteogenic lineage differentiation was induced and framed by the expression of RUNX2, a master transcription factor of osteoblastogenesis (Figures 2G and 4B-IV). RUNX2 shaped the differentiation route of mesenchymal stem cells into osteoblasts and activated the relevant gene expression (Figure 2G). Therefore, TGF-β signaling played an important role in modulating mesenchymal stem cell lineage selection and dictated the progression of mesenchymal differentiation into the osteogenic lineage by controlling the key transcription factor's expression and activities[25,44] (Figure 4B-IV). BMP signaling also insinuated mesenchymal stem cell differentiation and commitment via SMAD5 and the noncanonical pathway MAPK3, P38 MAPK, and JNK signaling.[51]

This study provides the first comprehensive exploration of the molecular mechanisms underlying the glioblastoma to gliosarcoma transformation. TGF-β signaling regulated the proneural–mesenchymal transition and drove the gliosarcoma differentiation into osteosarcoma modulated by RUNX2. We also elucidated the relationship between TGF-β and its downstream regulators and signaling pathways. Improved understanding of tumor transformation may enable early identification of tumors likely to undergo a subsequent transformation and these findings may contribute to the identification of novel therapeutic targets for this disease.

Supplementary material

Supplementary material is available online at *Neuro-Oncology* (https://academic.oup.com/neuro-oncology).

Keywords

glioblastoma | gliosarcoma | osteosarcoma | TGF-β signaling

Funding

This work was supported by the Intramural Research Program of the NIH, the National Cancer Institute, the Center for Cancer Research, the NIH-Oxford-Cambridge Scholars Program, and the University of Cambridge.

Conflict of interest statement

None declared.

Authorship statement

RNA-seq data analysis—A.L.; RNA extraction and sequencing—S.A., N.M.; wrote and edited the manuscript—J.H., A.L.; nanostring validation experiment—J.H., S.A.; sample collection for validation—N.B.; patient surgery—E.N.; patient clinical information—O.A.; pathology examination of the patient tumor samples—M.Q., S.K.; mutation analysis of the RNA-seq data—O.C.; project management—S.R., D.P., M.G.; concept initiation—M.G.

Data Availability

All data will be made available upon request.

References

1. Damodaran O, van Heerden J, Nowak AK, et al. Clinical management and survival outcomes of gliosarcomas in the era of multimodality therapy. *J Clin Neurosci*. 2014;21(3):478–481.
2. Han SJ, Yang I, Tihan T, Prados MD, Parsa AT. Primary gliosarcoma: key clinical and pathologic distinctions from glioblastoma with implications as a unique oncologic entity. *J Neurooncol*. 2010;96(3):313–320.
3. Cachia D, Kamiya-Matsuoka C, Mandel JJ, et al. Primary and secondary gliosarcomas: clinical, molecular and survival characteristics. *J Neurooncol*. 2015;125(2):401–410.
4. Verhaak RG, Hoadley KA, Purdom E, et al; Cancer Genome Atlas Research Network. Integrated genomic analysis identifies clinically relevant subtypes of glioblastoma characterized by abnormalities in PDGFRA, IDH1, EGFR, and NF1. *Cancer Cell*. 2010;17(1):98–110.

5. Koga T, Chaim IA, Benitez JA, et al. Longitudinal assessment of tumor development using cancer avatars derived from genetically engineered pluripotent stem cells. *Nat Commun.* 2020;11(1):550.
6. Frandsen S, Broholm H, Larsen VA, et al. Clinical characteristics of gliosarcoma and outcomes from standardized treatment relative to conventional glioblastoma. *Front Oncol.* 2019;9:1425.
7. Smith DR, Wu CC, Saadatmand HJ, et al. Clinical and molecular characteristics of gliosarcoma and modern prognostic significance relative to conventional glioblastoma. *J Neurooncol.* 2018;137(2):303–311.
8. Choi TM, Cheon YJ, Jung TY, Lee KH. A stable secondary gliosarcoma with extensive systemic metastases: a case report. *Brain Tumor Res Treat.* 2016;4(2):133–137.
9. Torp SH, Solheim O, Skjulsvik AJ. The WHO 2021 classification of central nervous system tumours: a practical update on what neurosurgeons need to know-a minireview. *Acta Neurochir (Wien).* 2022;164(9):2453–2464.
10. Cho SY, Park C, Na D, et al. High prevalence of TP53 mutations is associated with poor survival and an EMT signature in gliosarcoma patients. *Exp Mol Med.* 2017;49(4):e317.
11. Zhang G, Huang S, Zhang J, et al. Clinical outcome of gliosarcoma compared with glioblastoma multiforme: a clinical study in Chinese patients. *J Neurooncol.* 2016;127(2):355–362.
12. AlMuraikhi N, Almasoud N, Binhamdan S, et al. Hedgehog signaling inhibition by smoothened antagonist BMS-833923 reduces osteoblast differentiation and ectopic bone formation of human skeletal (mesenchymal) stem cells. *Stem Cells Int.* 2019;2019:3435901.
13. Raab P, Pilatus U, Hattingen E, et al. Spectroscopic characterization of gliosarcomas-Do they differ from glioblastomas and metastases? *J Comput Assist Tomogr.* 2016;40(5):815–819.
14. Hashmi FA, Salim A, Shamim MS, Bari ME. Biological characteristics and outcomes of gliosarcoma. *J Pak Med Assoc.* 2018;68(8):1273–1275.
15. Bani MA, Zehani A, Chelly I, et al. Gliosarcoma with smooth muscle cell differentiation: a case report. *Tunis Med.* 2016;94(4):337–338.
16. Oh JE, Ohta T, Nonoguchi N, et al. Genetic alterations in gliosarcoma and giant cell glioblastoma. *Brain Pathol.* 2016;26(4):517–522.
17. Barresi V, Cerasoli S, Morigi F, et al. Gliosarcoma with features of osteoblastic osteosarcoma: a review. *Arch Pathol Lab Med.* 2006;130(8):1208–1211.
18. Poyuran R, Bn N, Reddy YVK, Savardekar AR. Intraventricular gliosarcoma with dual sarcomatous differentiation: a unique case. *Neuropathology.* 2017;37(4):346–350.
19. Shukla S, Awasthi NP, Singh P, Husain N, Ojha BK. Gliosarcoma with leiomyomatous differentiation: a case report with an emphasis on histogenesis. *J Cancer Res Ther.* 2015;11(4):917–919.
20. Yao K, Qi XL, Mei X, Jiang T. Gliosarcoma with primitive neuroectodermal, osseous, cartilage and adipocyte differentiation: a case report. *Int J Clin Exp Pathol.* 2015;8(2):2079–2084.
21. Brennan CW, Verhaak RG, McKenna A, et al; TCGA Research Network. The somatic genomic landscape of glioblastoma. *Cell.* 2013;155(2):462–477.
22. Zaki MM, Mashouf LA, Woodward E, et al. Genomic landscape of gliosarcoma: distinguishing features and targetable alterations. *Sci Rep.* 2021;11(1):18009.
23. Kang SH, Park KJ, Kim CY, et al. O6-methylguanine DNA methyltransferase status determined by promoter methylation and immunohistochemistry in gliosarcoma and their clinical implications. *J Neurooncol.* 2011;101(3):477–486.
24. Wojtas B, Gielniewski B, Wojnicki K, et al. Gliosarcoma is driven by alterations in PI3K/Akt, RAS/MAPK pathways and characterized by collagen gene expression signature. *Cancers (Basel).* 2019;11(3):284.
25. Nagaishi M, Paulus W, Brokinkel B, et al. Transcriptional factors for epithelial-mesenchymal transition are associated with mesenchymal differentiation in gliosarcoma. *Brain Pathol.* 2012;22(5):670–676.
26. Hsieh JK, Hong CS, Manjila S, et al. An IDH1-mutated primary gliosarcoma: case report. *J Neurosurg.* 2017;126(2):476–480.
27. Alatakis S, Stuckey S, Siu K, McLean C. Gliosarcoma with osteosarcomatous differentiation: review of radiological and pathological features. *J Clin Neurosci.* 2004;11(6):650–656.
28. Barut F, Kandemir NO, Ozdamar SO, et al. Gliosarcoma with chondroblastic osteosarcomatous differentation: report of two case with clinicopathologic and immunohistochemical features. *Turk Neurosurg.* 2009;19(4):417–422.
29. Charfi S, Ayadi L, Khabir A, et al. Gliosarcoma with osteosarcomatous features: a short illustrated review. *Acta Neurochir (Wien).* 2009;151(7):809–813; discussion 813. discussion 813.
30. Lieberman KA, Fuller CE, Caruso RD, Schelper RL. Postradiation gliosarcoma with osteosarcomatous components. *Neuroradiology.* 2001;43(7):555–558.
31. Chen Y, Zhou S, Zhou X, et al. Gliosarcoma with osteosarcomatous component: a case report and short review illustration. *Pathol Res Pract.* 2022;232:153837.
32. Hanzelmann S, Castelo R, Guinney J. GSVA: gene set variation analysis for microarray and RNA-seq data. *BMC Bioinf.* 2013;14:7.
33. Subramanian A, Tamayo P, Mootha VK, et al. Gene set enrichment analysis: a knowledge-based approach for interpreting genome-wide expression profiles. *Proc Natl Acad Sci U S A.* 2005;102(43):15545–15550.
34. Wang Q, Hu B, Hu X, et al. Tumor evolution of glioma-intrinsic gene expression subtypes associates with immunological changes in the microenvironment. *Cancer Cell.* 2017;32(1):42–56.e6.
35. Ho XD, Nguyen HG, Trinh LH, et al. Analysis of the expression of repetitive DNA elements in osteosarcoma. *Front Genet.* 2017;8:193.
36. Zhou X, Fan Y, Ye W, et al. Identification of the novel target genes for osteosarcoma therapy based on comprehensive bioinformatic analysis. *DNA Cell Biol.* 2020;39(7):1172–1180.
37. Liu T, Papagiannakopoulos T, Puskar K, et al. Detection of a microRNA signal in an in vivo expression set of mRNAs. *PLoS One.* 2007;2(8):e804.
38. Li A, Walling J, Ahn S, et al. Unsupervised analysis of transcriptomic profiles reveals six glioma subtypes. *Cancer Res.* 2009;69(5):2091–2099.
39. Liu TM, Lee EH. Transcriptional regulatory cascades in Runx2-dependent bone development. *Tissue Eng Part B Rev.* 2013;19(3):254–263.
40. Corre I, Verrecchia F, Crenn V, Redini F, Trichet V. The osteosarcoma microenvironment: a complex but targetable ecosystem. *Cells.* 2020;9(4):976.
41. Plasari G, Calabrese A, Dusserre Y, et al. Nuclear factor I-C links platelet-derived growth factor and transforming growth factor beta1 signaling to skin wound healing progression. *Mol Cell Biol.* 2009;29(22):6006–6017.
42. Jazag A, Kanai F, Ijichi H, et al. Single small-interfering RNA expression vector for silencing multiple transforming growth factor-beta pathway components. *Nucleic Acids Res.* 2005;33(15):e131.
43. Labbe E, Lock L, Letamendia A, et al. Transcriptional cooperation between the transforming growth factor-beta and Wnt pathways in mammary and intestinal tumorigenesis. *Cancer Res.* 2007;67(1):75–84.
44. Roelen BA, Dijke P. Controlling mesenchymal stem cell differentiation by TGFBeta family members. *J Orthop Sci.* 2003;8(5):740–748.
45. Grafe I, Alexander S, Peterson JR, et al. TGF-beta family signaling in mesenchymal differentiation. *Cold Spring Harb Perspect Biol.* 2018;10(5):a022202.
46. Turini S, Bergandi L, Gazzano E, Prato M, Aldieri E. Epithelial to mesenchymal transition in human mesothelial cells exposed to asbestos fibers: role of TGF-beta as mediator of malignant mesothelioma development or metastasis via EMT event. *Int J Mol Sci.* 2019;20(1):150.
47. Wang H, Wu Q, Zhang Y, et al. TGF-beta1-induced epithelial–mesenchymal transition in lung cancer cells involves upregulation of miR-9 and downregulation of its target, E-cadherin. *Cell Mol Biol Lett.* 2017;22:22.

48. Rahman MS, Akhtar N, Jamil HM, Banik RS, Asaduzzaman SM. TGF-beta/BMP signaling and other molecular events: regulation of osteoblastogenesis and bone formation. *Bone Res.* 2015;3:15005.

49. Wu M, Chen G, Li YP. TGF-beta and BMP signaling in osteoblast, skeletal development, and bone formation, homeostasis and disease. *Bone Res.* 2016;4:16009.

50. Fedele M, Cerchia L, Pegoraro S, Sgarra R, Manfioletti G. Proneural–mesenchymal transition: phenotypic plasticity to acquire multitherapy resistance in glioblastoma. *Int J Mol Sci* . 2019;20(11):2746.

51. Zhang M, Yan Y, Lim YB, et al. BMP-2 modulates beta-catenin signaling through stimulation of Lrp5 expression and inhibition of beta-TrCP expression in osteoblasts. *J Cell Biochem.* 2009;108(4):896–905.